

Nano-diamond Coatings for Aluminum Substrates

Rodger Blum, Dinesh Kalyana-Sundaram, Rajeev Nair, Pal Molian

Department of Mechanical Engineering
Laboratory for Lasers, MEMS, and Nanotechnology
Iowa State University
Ames, IA 50011-2161

ABSTRACT

Laser-induced phase transition and sintering of nano-diamond powders (4-8 nm) was used to produce a thick (10-50 μm) strongly adherent nano-diamond/diamond-like carbon (nD-DLC) coatings on aluminum alloy 319. Nano-diamond powders produced by detonation synthesis were electrostatically sprayed on the aluminum substrate coupons followed by a continuous wave CO_2 laser heating in a controlled fashion to cause a liquid-phase nano-sintering which yielded a strongly adherent coating. A transition to diamond-like carbon produced a Vickers hardness of 2250 kg/mm^2 , and a transition to complete nano-diamond produced a Vickers hardness of 9000 kg/mm^2 . The potential application of the work is hard and wear resistant coatings for light-weight engine components to improve their wear resistance.

Keywords: nanocoatings, diamond, tribology, aluminum, laser sintering

1 INTRODUCTION

Diamond is the hardest material known and finds great number of applications because of its unique and attractive physical and chemical properties. In addition to its super hardness, it also exhibits chemical inertness, higher wear resistance, and higher thermal conductivity. Nano-diamond is emerging as a new type of material with even better properties than single and poly crystalline diamonds. Commercially produced nano-diamond powders are used in various applications including abrasives for the optical and semiconductor industries, for durable and hard coatings, polymer reinforcements, lubricant additive for engines and other moving parts, protein absorbent and even medicinal drugs [1-4]. Nano-diamond powders are also being used for making new types of rubber and are important components in reprocessing worn tire rubber [1]. Nano-diamond coatings are generally synthesized by chemical vapor deposition (CVD) and plasma deposition techniques. These techniques are bound by time and cost constraints, and can be hazardous. The gases used during the chemical vapor deposition can be toxic, flammable, corrosive, and even explosive [5]. The high cost of chemical vapor deposition and plasma deposition is because of the need for a vacuum to create the plasma and then the reactor used needs to be more sophisticated to

contain the plasma [5]. Other downfall to the plasma deposition process is that its capability of high energy plasma could damage the substrate [5]. The time constraint can be seen in these processes by the fact that the fastest growth rate seen is 900 μm per hour but at this speed nothing was said about the uniformity of the layer, its nucleation density, and the stability of the operation [6]. A more typical growth rate would be .5-5 μm per hour; there are a few instances of 20 μm per hour in the plasma enhanced CVD process [6, 7]. So the CVD process is relatively slow.

In this work, we developed novel techniques to achieve nano-diamond coatings on aluminum A319 by CO_2 laser-sintering process. Aluminum alloy A319 is a widely used material in the production of automotive components due to its excellent mechanical properties and good castability characteristics [8]. Laser sintering technique is the continuous rastering of the laser beam on the sample surface. Laser sintering is a widely used technique for many rapid proto-typing processes including selective laser sintering (SLS) [9, 10], and laser engineered net shaping (LENS). These processes are layered based meaning that they make parts layer by layer [9, 10]. In the selective laser sintering process a layer of powder is spread over the previous layer and sintered to that layer by a raster filling motion of the laser [9, 10]. The layer of powder is only about as thick as the particle size of the powder being used [9, 10]. In our experiments, laser sintering is used to bond a thick (25-35 μm) layer of nano-diamond powder to an aluminum substrate. A continuous wave CO_2 laser (10.6 μm) was used for this process. The goal of the experiment is to strengthen the surface hardness of the aluminum by laser inducing a phase transition of nano-diamond powder and then sintering it to the substrate. This nano-diamond coating should make the aluminum more durable with less friction. The success of the project could help us in developing longer life engine components.

2 EXPERIMENTAL DETAILS

2.1 Preparation of Nano-diamond Powders

Nano-diamond powders of 4-8 nm were produced by shock detonation synthesis and were confirmed from TEM images. In the detonation synthesis process, powerful explosives are mixed with the composition $\text{C}_a\text{H}_b\text{N}_c\text{O}_d$ with a negative oxygen balance in a non-oxidizing medium to yield

condensed carbon phase that involves nano-diamond particles [1]. The result of this process be 75% nano-diamond powder [1]. A cleaning process is done to the resultant powder to remove almost all of the impurities. The nano-diamond powder used in this experiment had no more than 2% impurities.

2.2 Preparation of Aluminum Coupons

Aluminum ingot of A319 was purchased from Custom Alloy Light Metals. The composition of A319 can be seen in Table 1 and it conforms to the ASTM specifications. Rods of 25 mm (~1”) dia x 250 mm long (~10”) were prepared from the ingot by die casting. After the aluminum was cast into rods it was heat treated to convert it to 319-T6. T6 has a higher tensile strength. Following the heat treatment, the aluminum was then cut into coupons/discs of approximately 3.2 mm (1/8”) thickness. Once in coupon form the disk surfaces needed a good surface finish. To accomplish this a Clemco Industries Dry Blast Cabinet with Dust Collector (Model ACDFM) was used to sandblast the surfaces.

Table 1: Composition of A319

| Element | WT % | Element2 | Wt %3 |
|---------|-------|----------|--------|
| Si | 5.860 | Ti | 0.160 |
| Fe | 0.678 | Sn | 0.021 |
| Cu | 3.519 | Pb | 0.032 |
| Mn | 0.246 | Ni | 0.121 |
| Mg | 0.056 | OET | < .500 |
| Cr | 0.104 | Sr | 0.000 |
| Zn | 0.901 | Al | 87.8 |

2.3 Electrostatic Spray Coating

After the aluminum A319 coupons were made, nanodiamond were electrostatically spray coated on one of the surfaces of the coupon. The deposition of nanodiamond powder was done by a home-built corona charging based electrostatic spray coating setup. The powder was deposited by first being negatively charged. Once charged the nano-particles follow the electric field lines toward the grounded substrate (aluminum), forming a uniform coating. The coating is loosely adhered to the substrate by electrostatic forces which may cause the coating to decay as the electrostatic forces dissipate. Since the size of the diamond particles are in the order of nanometers, agglomeration of the particles is a potential issue that has to be overcome to achieve uniform deposition. To prevent agglomeration of the particles, a jet mill was integrated into the electrostatic spray coating setup (Fig 1). Besides the physical properties of the powder (particle density, particle shape, average particle size, particle size distribution, and dielectric properties), process parameters including electrode-substrate distance, electrical voltage applied at the electrode, and the main air pressure affect the formation of the coating. A coating of 25-35 μm

was obtained at a voltage of 60 kV with the electrode to substrate distance of 150 mm.

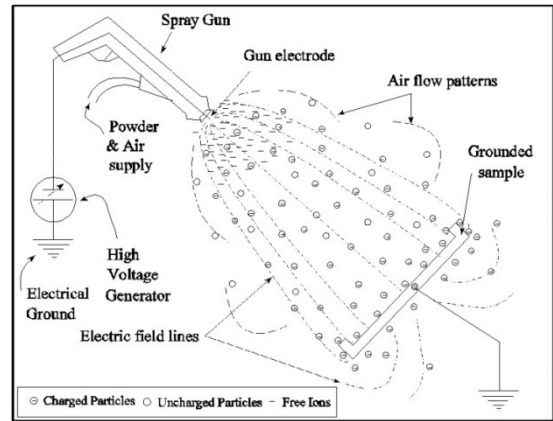


Figure 1: Schematic of the electrostatic spray coating

2.4 Laser Sintering Setup

A 1.5 kW Continuous wave CO₂ laser (Spectra Physics – 820) of 10.6 μm wavelength with CNC controlled worktable was used for experiments as shown in Fig 2. The coupons were held in place by means of a vice clamped on to the table. Sintering was performed using a focused beam of 0.2 mm spot size with an overlap of 5% between passes. A lens of 127 mm (5”) focal length helped in achieving the desired spot size. Argon gas at $2.3 \times 10^{-2} \text{ m}^3/\text{s}$ (50ft³/min) was used as an assist gas during the sintering process. Argon is used as an assist gas because it prevents oxidation as it is an inert gas [11]. Since it is an inert gas it would not interact with the liquid melt metal at the laser-substrate interface [11]. Preliminary studies of single pass treatment were made to identify the best set of parameters for laser-sintering. After identification, laser sintering was performed to completely cover the surface of the coupon in a raster-frame motion and it took 70 passes for sintering to be completed.

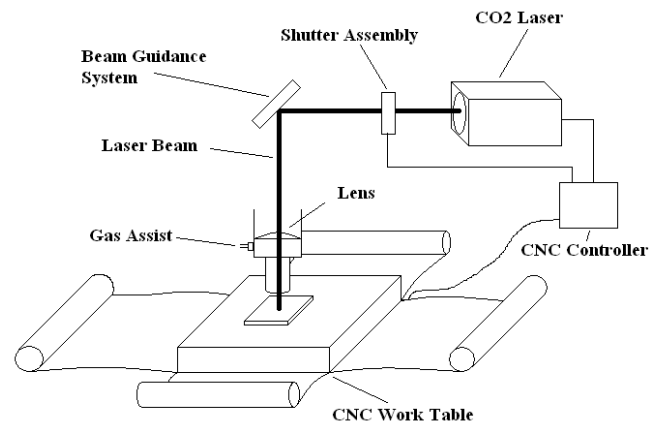


Figure 2: Schematic of the laser sintering setup

2.5 Measurement Techniques

To identify the mechanical and tribological properties of the finished coating the following tests were performed: hardness by Vickers micro-hardness test, identification of the carbon phase by Raman Spectroscopy, friction and wear test, and surface roughness measurement by optical profilometer. The micro-hardness of the heat treated aluminum is known to be around 113 kg/mm^2 but this can vary depending on the temperature it is held at [12]. Again the goal is find the hardness to be between $2000\text{-}9000 \text{ kg/mm}^2$. Following the hardness tests, the surface will be characterized using a Renishaw inVia Raman Microscope at a wavelength of 488 nm . With this process we are expecting to get a surface that consists of a mixture of nano-diamond, diamond-like-carbon, and graphite. These three carbon phases will yield three very different Raman peaks. Diamond will give a definite peak at 1332 cm^{-1} , and graphite will yield a definite peak at 1580 cm^{-1} , while diamond like carbon can yield a range of peaks but the main peak is at 1355 cm^{-1} [13]. Thus Raman Spectroscopy will be plotted through the range of $1100\text{-}2000 \text{ cm}^{-1}$.

3 RESULTS AND DISCUSSION

3.1 Effect of Laser Parameters

Laser powers in the range $200 \text{ W}\text{-}1000 \text{ W}$ were studied. Higher powers than 400 W caused vaporization of the coating. Lower powers than 200 W did not cause melting of the substrate which is necessary for liquid phase sintering. Parameter studies coupled with Raman spectroscopy yielded the most optimum parameters at 200 W and 85 mm/sec (200 in/min). Fig 3 shows the nano-diamond covered coupon.

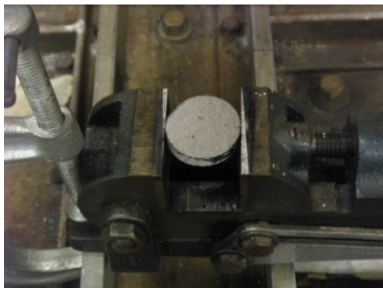


Figure 3: Coupon sintered with optimal parameters

3.2 Cleaning the Samples

Ultrasonic water cleaning was found to remove the outer layer of carbon that was produced during laser sintering. At first this layer was found to be easily scratched away and was thought to damage the Raman test we were taken. The coupons were cleaned in an ultrasonic bath for 3 minutes using deionized water. The samples were then removed from the bath and left to air dry. It was found that cleaning of the coupon gave better Raman peaks.

3.3 Hardness Tests

A Wilson Tukon Microhardness Tester (Model 200) was used in taking Vickers micro-hardness tests. These tests were done using a 25 gram weight which is better for superficial layers and avoids the risk of puncturing the coating. The Vickers hardness tests were used as a basis for characterizing the process parameters. The uneven spread of the nano-diamond powder after laser-sintering resulted in a rougher surface. The rougher surface profile combined with the higher hardness of the diamond particles makes it difficult to clearly identify the endpoints of the indentation caused by the instrument probe. Along with the micro-hardness test, a macro hardness test was also done. In this test a Leco Hardness Tester (RT-120) with a test weight of 15kg was used. Fig. 4 shows the results of plain aluminum coupon and a coupon with the coating on it. This was done to see the results of the test. As shown by the figure there is not much difference between the two surfaces, which is not what was expected. If there was a difference in the two surfaces, we expected there to be some chip formation or something around the indentation of the coated sample. Since we were neither able to get an accurate micro-hardness nor macro hardness reading, we decided to use Raman Spectroscopy for determining what laser parameters yield the best result.

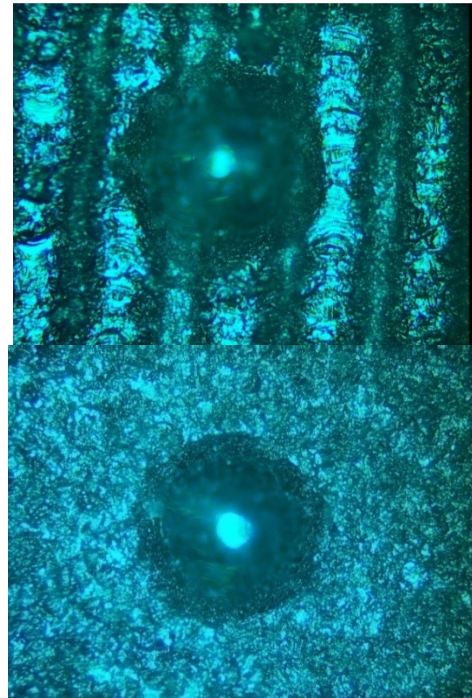


Figure 4: (Top) Coated Aluminum Sample (Bottom) Plain Aluminum Sample

3.4 Raman Spectroscopy

Raman Spectroscopy of the single-pass parameters which were done at 200 W and a 1000 W with a range of laser speeds. These powers were chosen to understand the effect of lower and higher powers. Also 1000W would yield an

interface temperature ($> 900^{\circ}\text{C}$) high enough to melt the aluminum which will enable sintering of the nano-diamond powders to take place. We observed no definite diamond peaks at 1332 cm^{-1} in the Raman analysis of the laser sintered coupons both at 200 W and 1000 W. We also observed rounded peaks of diamond like carbon and graphite at 1350 cm^{-1} and 1550 cm^{-1} . We even had a spectrum that carried one big peak from about 1350 to 1550 cm^{-1} . A higher graphite count was noticed which might primarily be due to the high heat created at 1000 W except at high speeds of nearly 245 mm/s (600 inch/min). At high speeds the spectra showed some diamond-like carbon (peak at 1350 cm^{-1}) starting to appear but the graphite peak count was still higher. From the tests conducted we narrowed down the laser parameters by comparing the intensity of diamond, diamond-like carbon, and graphite peaks. The parameter that gave us the best result was 200W at 84.7 mm/s (200 in/min), and we used these parameters to laser sintered the whole surface of the coupon. Raman Spectra of both the laser-sintered sample and nano-diamond powder can be seen in Fig 5. The spectrum shows an upward slope, but our focus is on the two peaks in the center of the spectrum. These are the diamond like carbon and graphite peaks. The figure shows that the intensity of the peaks is higher than that found in the original nano-diamond powder.

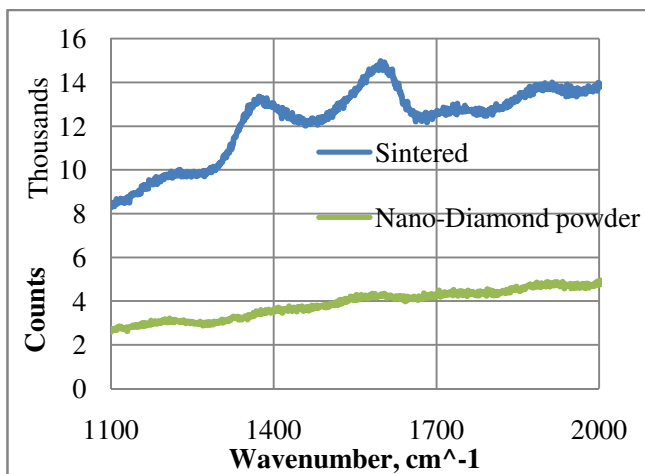


Figure 5: Spectra of the optimal parameters and nano-diamond powder.

3.5 Friction and Wear

Friction was measured using a custom-built reciprocating ball-on-flat microtribometer that can produce a microscale (apparent area $\sim 1000\text{ }\mu\text{m}^2$) multi-asperity contact [14]. The details of equipment are found elsewhere [14]. In short, the microtribometer uses a spherical probe placed at the end of a crossed I-beam structure, which is lowered using a linear stage to apply a desired normal load to the sample. The normal and friction (lateral) forces are measured using semiconductor strain gages on the cantilevers. Friction forces can be resolved to approximately $\pm 5\text{ }\mu\text{N}$ and normal forces to approximately $\pm 15\text{ }\mu\text{N}$. All samples were cleaned with DI water in an ultrasonic bath for 3 min and dried using dry air

prior to tests. To obtain the coefficient of friction, ramped load tests were performed in which the load was increased linearly with the sliding distance. An AISI 52100 steel ball of radius 1.2 mm and RMS roughness of 4 nm was used to probe test the coupon. The load was increased from 0.2 to 200 mN as the probe was moved across a stroke distance of 45 mm at 10 mm/s. The average friction coefficient of the bare aluminum and nano-diamond sintered aluminum was 0.13 and 0.22 respectively. The friction tests were performed at room temperature of 24°C and 30% relative humidity.

A 100 cycle reciprocating sliding wear test was performed under the same friction test conditions at a constant load of 100 mN and a stroke speed of 5 mm/s for a total sliding distance of 8 m (80 mm/cycle). Wear track profiling was carried out using an optical profilometer. The wear depth of bare aluminum was around $3\text{ }\mu\text{m}$ and that of nano-diamond coated aluminum was around $8\text{ }\mu\text{m}$. The wear tests done on the nano-diamond coated aluminum are not accurate due to the ridges on the coupon. The 1.2 mm radius steel ball probe used in the test was not small enough to pass between the ridges. Hence during the test, the probe was sitting between two ridges there by wearing both ridges down before reaching the surface of the coupon. The measurement of wear of $8\text{ }\mu\text{m}$ includes both the ridge height ($\sim 5\text{-}6\text{ }\mu\text{m}$) and the depth worn into the surface. Therefore more work needs to be done to improve the surface quality so that accurate tests can be done.

Surface roughness was also measured with the optical profilometer. The measurements for this test were done on the laser path (parallel to the ridges). We found the surface roughness of the nano-diamond coated coupon to be $2.4\text{ }\mu\text{m}$. This result is a little higher than that of the bare aluminum which was found to be $1.4\text{ }\mu\text{m}$. This shows that if we can produce a coupon without ridges, the resulting surface roughness would be equivalent to the original substrate.

4 CONCLUSION

We have investigated a laser-based coating technique of nano-diamond particles on aluminum substrate. The coating consisted of nano-diamond, diamond-like carbon and graphite phases with reasonable adherence of the nano-powder to the substrate. However, we were unable to measure hardness equivalent to that of the nano-diamond for the following reasons/constraints. Rastering was done to achieve a complete coverage of the surface of the coupon due to focused spot sizes ($\sim 200\text{ }\mu\text{m}$) used (5% overlap in between passes). This resulted in uneven surfaces vowing to higher surface roughness, higher friction coefficient, and difficulty in measuring surface hardness. This can be avoided if we could use a larger focus spots and a larger spot size will also help to reduce number of rastering passes. Further studies are being conducted to understand the feasibility of using larger spot sizes. We will also explore the use of gold plated sample holder with DI water to get more explicit Raman spectrum.

Acknowledgements

The authors would like to thank the National Science Foundation for the Grant 0738405. We also appreciate Dr. Anatolli Frishman for acquiring the nano-diamond powder for us, Mr. Wenping Jiang for electrostatically spray coating our samples & providing the information on the setup, and Mr. Hal Sailsbury for his help in characterizing the surface after sintering. We would also like to thank Mr. Satyam Bhuyan (Mechanical Engineering, Iowa State University) and Mr David Eisenmann (Scientist, Center for Non-destructive Testing, Iowa State University) in helping us to measure tribological properties and surface roughness.

REFERENCES

- [1] V.Y. Dolmatov, "Detonation synthesis of ultradispersed diamonds: properties and applications," *Russian Chemical Reviews*, 70, 607-626, 2001.
- [2] G. Post, V.Y. Domatov, V.A Marchukov, V.G. Sushchev, M.V. Veretennikova, and A.E. Sal'ko, "Industrial synthesis of ultradisperse detonation diamonds and some fields of their use," *Russian Journal of Applied Chemistry*, 75, 755-760, 2002.
- [3] G.P. Bogatyreva, M.A. Marinich, N.A. Oleynik, and G.A. Bazaliy, "Nanodispersed Diamond Adsorbents for Biological Solution Cleaning, in Nanostructured Materials and Coatings for Biomedical and Sensor Applications," Kluwer Academic Publishers, 111-119, 2002.
- [4] G.P. Bogatyreva, M.A. Marinich, and V.L. Gvyazdovskaya, "Diamond- an adsorbent of a new type," *Diamond and Related Materials*, 2002-2005, 2000.
- [5] K.L. Choy, "Chemical vapour deposition of coatings," *Progress in Materials Science*, 48, 57-170, 2003.
- [6] W. A. Yarbrough, and Russell Messier, "Current Issues and Problems in the Chemical Vapor Deposition of Diamond," *Science*, 247, 688-696, 1990.
- [7] J.C. Angus and Cliff C. Hayman, "Low-Pressure, Metastable Growth of Diamond and Diamond-like Phases," *Science*, 241, 913-921, 1988.
- [8] E. Cerri, E. Evangelista, S. Spigarelli, P. Cavaliere and F. DeRiccardis, "Effects of thermal treatments on microstructure and mechanical properties in a thixocast 319 aluminum alloy," *Materials Science and Engineering*, 284, 254-260, 2000.
- [9] J.P Kruth, X. Wang, T. Laoui and L. Froyen, "Lasers and materials in selective laser sintering," *Assembly Automation*, 23, 357-371, 2003.
- [10] D.T. Pham, S. Dimov, F. Lacan, "Selective laser sintering: applications and technological capabilities," *Proceedings of the Institution of Mechanical Engineers*, 213, 435-449, 1999.
- [11] D.K.Y. Low, L. Li and A.G. Corfe, "The influence of assist gas on the mechanism of material ejection and removal during laser percussion drilling," *Proceedings of the Institution of Mechanical Engineers*, 214, 521-527, 2000.
- [12] R. Mahmudi, P. Sepehrband and H.M. Ghasemi, "Improved properties of A319 aluminum casting alloy modified with Zr," *Materials Letters*, 60, 2606-2610, 2006.
- [13] A.C. Ferrari and J. Robertson, "Raman spectroscopy of amorphous, nanostructured, diamond-like carbon, and nanodiamond," *Philosophical Transactions of the Royal Society of London*, 362, 2477-2512, 2004.
- [14] Bhuyan, S., et al., "Boundary lubrication properties of lipid-based compounds evaluated using microtribological methods," *Tribology Letters*, 22(2), 167-172, 2006.